Proceedings of the
International Conference on Mechanical Engineering 2005
(ICME2005) 28 - 30 December 2005, Dhaka, Bangladesh

ICME05-AM-37

STUDY ON THE UNLOADING MODULUS OF AL-ALLOY FOAM BY FE MODELING

A. Kim*, **K. Tunvir and S. S. Cheon**

Division of Mechanical Engineering, Kongju National University
Shinkwan-dong 182, Kongju, Chungnam 314-701, Korea (South)
*Email: amkee@kongju.ac.kr

ABSTRACT

Behavior of unloading modulus of closed cell Al-alloy foam produced by melt based process has been studied through experiment and finite element (FE) analysis. The elastic modulus under monotonic compression has been found to increase with increment of strain. FE analysis of monotonic compression was accomplished with a multiple lattice FE model in which each unit lattice is composed of cubic and spherical structured cells. The unloading behavior of the monotonic compression in FE analysis also showed the same trend as in the experiment but with a discrepancy in low deformation range. This discrepancy may be associated with the different cell morphologies which caused the different deformation patterns of the cells. The influence of the loading condition on the unloading modulus was also studied by performing a compression-compression fatigue test and measuring the unloading modulus using the cyclic stress-strain during each fatigue cycle. The unloading elastic modulus in fatigue showed a decreasing trend with increase of strain unlike in case of the monotonic compression.

Keywords: Aluminum alloy foam, Elastic modulus, Monotonic compression, Fatigue.

1. INTRODUCTION

The recent development in the cost effective processes for making metallic foam has increased the prospective application of metal foam in sandwich panel for light weight structural components, in energy absorption systems for protection from impacts, in heat sink for electronics devices and in acoustic insulation. These applications require a thorough knowledge of the foam properties especially the compressive strength, elastic modulus, relative density, morphology etc. In this study we report on unloading modulus of aluminum alloy foam produced by the melt based techniques.

The elastic modulus and compressive strength of Shinko wire, Fraunhofer and Mepura commercial foams have been measured in a number of studies [1- 4]. Results of several of these showed the natural behavior of normalized elastic modulus with the variation of relative density. While the values for the normalized parameters, assessed by Simon and Gibson [2], unveiled that the unloading elastic modulus of Alporas, Alcan and Alulight foams are significantly higher than the initial loading modulus, suggesting that local yielding occurs almost immediately on loading. The effect of cell wall curvature and corrugation on the modulus has been investigated [3] through FEM analysis of periodic unit tetrakaidecahedral cell [4] in which the result revealed that the cell wall curvature and the corrugation may account for up to a 70% drop in modulus of some Al foams below the ideal values estimated for the planar cell walls. However not many have been accomplished to identify the behavior of elastic modulus of metallic foam at various deformations after the yielding.

In the current study the behavior of unloading modulus of Al-Si-Ca alloy foam having an isotropic material property and pure ductile nature was investigated by experiment and finite element analysis. The multiple cell FE model having the unit cell morphology as cubic-spherical section arrangement was used. As the cell wall morphology and deformation nature directly influence the unloading behavior, the heterogeneity was considered in the FE model through varying the relative density statistically in the model. The unloading modulus from finite element analysis showed the same trend as found from experiment. The effect of loading condition on the unloading modulus was investigated also through compression-compression fatigue test and behavior of unloading modulus was found to be unlike that from monotonic compression test.

2. EXPERIMENT

2.1 Material and Specimen

The Al-Si-Ca alloy foam was produced through the melt based process by the commercial manufacturer, FoamTech, Korea and was obtained in the form of panel of size 600 x 1200 x 35 mm. The processing route of this

is proprietary; hence it is not unveiled here. The FOAMTECH foam has a relatively uniform microstructure and is available in a large range of cell size depending upon the relative density. The foam used in this study had the average cell diameter of about 4-5 mm and the relative density 12 %. Skin was removed from these foams and specimens were cut to the appropriate dimension (35 x 35 x 40 mm) using electrical discharge cutting machine with a guide to ensure that the cuts were made accurately and straight. Such a dimension was chosen so that the edge length of the foam specimen in all cases be at least 7 times the cell size. This is required to avoid the edge effect which may reduce the measured values of elastic modulus and compressive strength. [5]

2.2 Monotonic Compression Test

An MTS 810 machine was used to perform the uniaxial compression test. The load and the displacement were monitored by a computer equipped with a data acquisition system. In the test the load was applied at a constant displacement speed of 0.02 mm/s and the specimens were compressed between parallel steel platens to ensure a perfect axial loading. Compression was stopped when 85% strain was reached. The unloadings were carried out at various strain level by periodically interrupting the test at 5%, 10%, 15%, 20%, 25%, 30%, 35%, 40% and 45% strain respectively where the specimens were unloaded approximately up to 10% of the applied load and the unloading data were recorded.

2.3 Fatigue Test

Fatigue test was performed at load ratio R of 0.1 and an endurance ratio (maximum fatigue load / plateau stress) of 0.8. The test frequency was 5 Hz. In the fatigue test it was seen that shortening of specimen took place with the increasing number of cycle. However, an incubation period is evident, for any endurance ratio, at the end of which the rate of shortening is accelerated abruptly. This sudden rise of the rate of progressive shortening takes place at a strain level approximately 4% which was nearly equal to the monotonic yield strain of the foam. The unloading modulus in the fatigue test was measured by measuring the cyclic stress and strain during each fatigue cycle.

3. MODEL FOR FE ANALYSIS

3.1 Geometry of the Unit Lattice

The FE model is assumed to be composed of densely packed lattices of small and large cells while each unit lattice possesses cubic and spherical sections such that cubic and spherical sections produce large and small cells respectively when comprises with the neighboring sections. The morphology of the cells arrangement and isometric view of the unit lattice with neighboring lattices can be observed in Fig. 1 The walls of the small cells are assumed to be thicker than those of the large cells (Fig. 1) in the FE model based on the micro structural examination of real Al-Si-Ca alloy foam. The details of the unit lattice for FE model and derived geometrical relations can be found in reference [6, 7]. From the geometrical relation, the relative density (ρ_f / ρ_s) of a cubic lattice can be determined by the volume

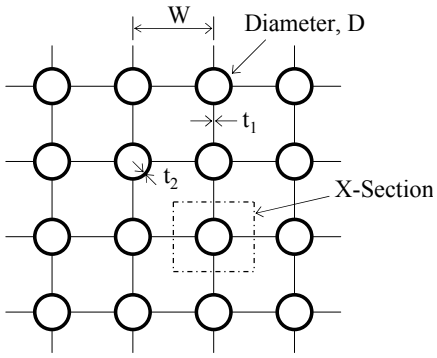

(a)

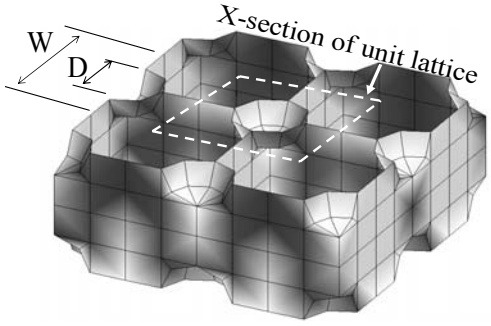

(b)

Fig 1. Structure of the cubic-spherical model; (a) Cell arrangement and wall thickness morphology, (b) Isometric view of the unit lattice with neighboring lattices

fraction of skeleton in the cube as follows:

$$\frac{\rho_f}{\rho_s}=3\left[1-\frac{\pi}{4}\left(\frac{D}{W}\right)^2\right]\left(\frac{t_1}{W}\right)+\frac{1}{6}\pi\left[6\left(\frac{D}{W}\right)^2+12\left(\frac{D}{W}\right)\left(\frac{t_2}{W}\right)+8\left(\frac{t_2}{W}\right)^2\right]\left(\frac{t_2}{W}\right) \quad (1)$$

Where t_1 and t_2 are the thicknesses of the cruciform and spherical sections in the unit lattice respectively, W is the width of lattice, and D is diameter of the spherical section. The relative density is defined as ρ_f / ρ_s where ρ_f and ρ_s are density of the foam and the density of solid from which the foam was made respectively. The ratio D/W, called cell size ratio, was set to 0.4646 and t_2/t_1, called thickness ratio, was set to 2.5 for the FE model which were calculated from the relative density and measured cell geometry of the real foam specimen. The detail description of this calculation can be found in [6]. In the model the value that used for thickness ratio (t_2/t_1) was greater than 1, indicating that the spherical cells (small cells of the foam) are thicker than cubic cells (large cells). For this Al-Si-Ca alloy foam, ρ_s was taken as the mass density of solid aluminum 2.89 g /cm^3.

3.2 Inhomogeneity in the Foam Model

Real foams always possess some heterogeneity like

large pores, broken cell walls, voids, presence of second phase particles etc. The finite element model was assumed to be globally isotropic in nature while possessing heterogeneity. The local heterogeneity represents the density variation of the unit cells. These heterogeneities in the FE model are assumed to be the function of the cell wall thickness and are implemented

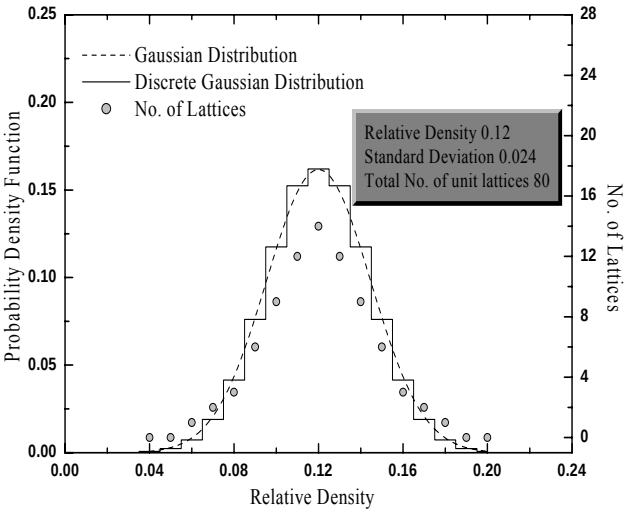

Fig 2. Satistical distribution of relative density among the unit lattices of FE model and corresponding number of unit lattices to each distributed density level

in the model by varying the relative density statistically among the unit lattices of the model (using eq. 1). The probabilistic distribution of the cell density in the model was assumed to possess a standard deviation of 0.2 times the mean value, which might represent the variation in cell density and internal defects, such as porosities, second phase particles and inclusions [8]. The unit cells with different densities were randomly distributed in the model for which a random number table [9] was used in which the digits occur randomly and each time with equal probability. The multiple cells model consisted of 80 unit cells (4 units x 4 units x 5 units) in total. Fig. 2 shows the discrete Gaussian distribution of relative density of the cells assumed for the multiple cells finite element model along with the distribution of number of cells corresponding to each distributed density level.

3.3 FE Model

The FE model for cubic-spherical foam was designed and analyzed by the nonlinear explicit FE code LS-DYNA (3D). The complete FE model used for the analysis of compressive behavior of Al-alloy foam is shown in Fig. 3 The model consists of 80 unit (4 units X 4 units X 5 units) lattices. The four node Belitschko Tsay Lin shell element was used with six degree freedom per node. A piecewise linear plasticity material model of LS-DYNA 3D material library was used. The contact between the upper surface of the FE model and the compression platen was simulated with automatic surface to surface contact while automatic single surface contact was introduced to capture all the contact interactions in the model during plastic deformation. One degree translational movement of the top surface was allowed along with the five degree constraints while six degree constraints were applied to the bottom of the model. The constitutive relation for foam cell wall material that used in the FE analysis of the foam model was evaluated through nanoindentation methodology on the thin cell wall of foam [10]. The evaluated material properties were as E = 78 GPa, σ_y = 84.61 MPa and strain

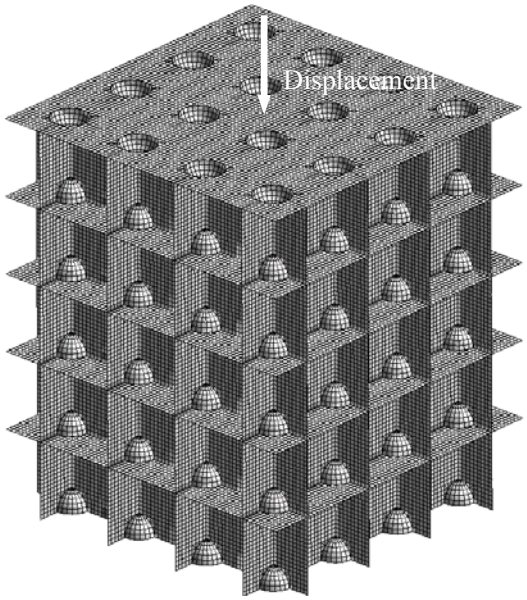

Fig 3. Multiple cell finite element model

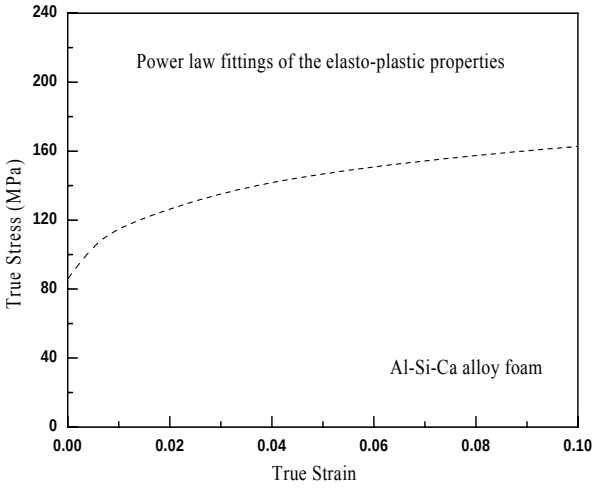

Fig 4. The stress-strain curve of alloy Al-Si-Ca cell wall obtained from nanoindentation method

hardening exponent n = 0.12. Fig. 4 is showing power law fittings of the evaluated material properties for the cell wall material of Al-Si-Ca alloy foam.

4. RESULTS AND DISCUSSION

4.1 Result from Compression and Fatigue Test

The stress-strain curve of Al-Si-Ca alloy foam having relative density 12% from monotonic compression test is shown in Fig. 5 The curve shows an initial linear elastic

region where partially reversible cell wall bending occurs, followed by a plastic plateau stress at which successive bands of cells collapse, buckle and yield, and finally a densification region where the stress raise sharply as complete compaction commences. At 3% strain, the unloading stress-strain curve showed an elastic modulus of 150 MPa while the plastic plateau strength of the foam obtained from the monotonic compression test was 2.88 MPa. The unloading curves of

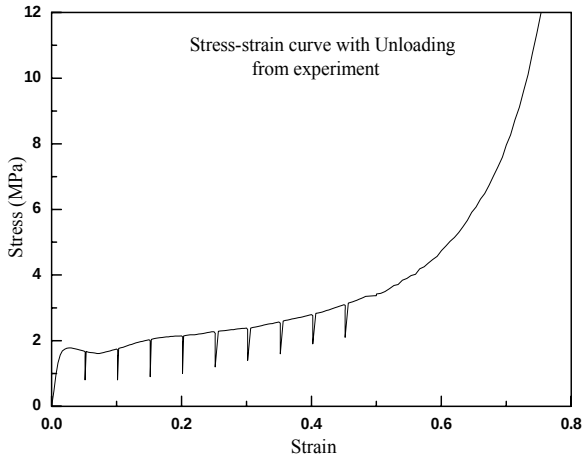

Fig 5. Stress-strain curve of Al-Si-Ca alloy foam under monotonic compression

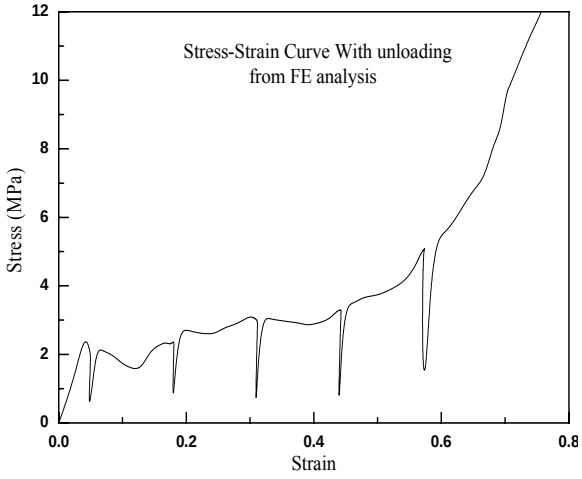

Fig 6. Stress-strain curve for Al-Si-Ca alloy foam obtained from FE analysis

the foam showed much steeper slopes than the loading curve. The unloading moduli were calculated from the change in axial strain corresponding to the 10% drop in the load. The simulation was carried out with a thickness ratio (t_2/t_1) of 2.5 between cubic and spherical section which give good stress-strain agreement with experiment. Fig. 6 shows the stress strain curve having unloading obtained from simulation in which unloading data were taken at the strain 5%, 18%, 25%, 42% and 57%. Comparing the Figs. 5 and 6 it can be seen that the initial yielding and compressive strength obtained from the experimental result lie below the result obtained from simulation suggesting that the other types of irregularity like evidence of large pores, brittle fracture of cell walls, and presence of second phase particles etc. which prevail in the real foam regularly also play a role.

The strain versus number of cycle data in compression-compression fatigue test for Al-Si-Ca alloy foam measured with a load ratio R = 0.1 and endurance ratio $\sigma_{max} / \sigma_{pl} = 0.8$ are shown in Fig. 7. Whilst in Fig. 8 the behavior of unloading modulus measured at various

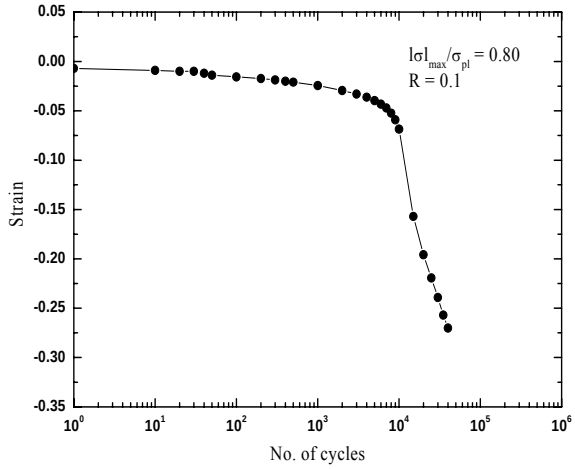

Fig 7. Shortening of foam specimen at various cycle under compression-compression fatigue

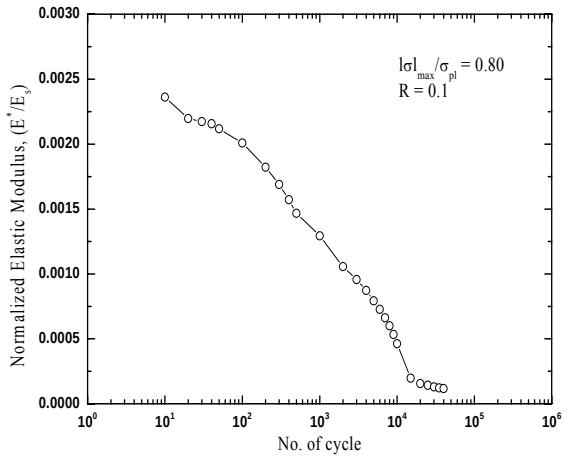

Fig 8. Measured unloading modulus at various cyclic strain

cycles is shown. The unloading modulus in fatigue was measured by measuring the cyclic strain during each fatigue cycle. It is evident from the figure that the strain increases with the number of cycle indicating that the shortening of the specimen takes place with the increasing number of cycle. However the incubation period was occurred at about 10^4 cycles for $\sigma_{max} / \sigma_{pl} = 0.8$. The unloading modulus decreases gradually with increasing number of fatigue cycle.

4.2 Behavior of Unloading Modulus Under Different Loading Condition

Unloading elastic modulus E of monotonic compression and compression-compression fatigue normalized by the initial value E_o (0.22 GPa in fatigue) are compared in Fig. 9. It is seen that the value of elastic

modulus of Al-Si-Ca alloy foam decreases sharply with increasing strain in case of fatigue compression, while in case of monotonic compression the value of elastic modulus rather increases with the strain. The simulation result of monotonic compression also shows an increasing trend with strain indicating that the multiple lattices finite element model may predict the behavior of closed cell aluminum alloy foam well. From the deformation patterns of real foam specimens in case of monotonic compression [Fig. 10 (a)] it can be revealed that the spherical cells of the foam are first bended plastically and take the elliptical shape which is stiffer and more stable in nature than the original cell, and then enter into densification with further compression. As it is heading to the densification, progressively it becomes foam with higher density whose cells are shrunken in shape. As the higher density foam shows the higher stiffness, the unloading elastic modulus [11] of the foam is increasing with strain. Besides, up to 45% strain the values of unloading elastic modulus obtained from simulation lie below those obtained from monotonic compression test. Within 60% strain the largest difference between two values of modulus at the same strain was about 9% of experimental value obtained from monotonic compression test. This discrepancy might be

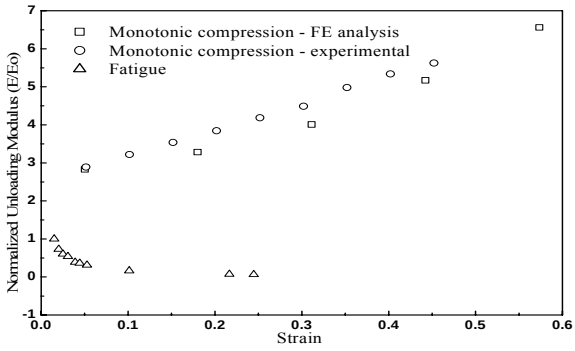

Fig 9. Behavior of unloading modulus at various strains under different loading condition

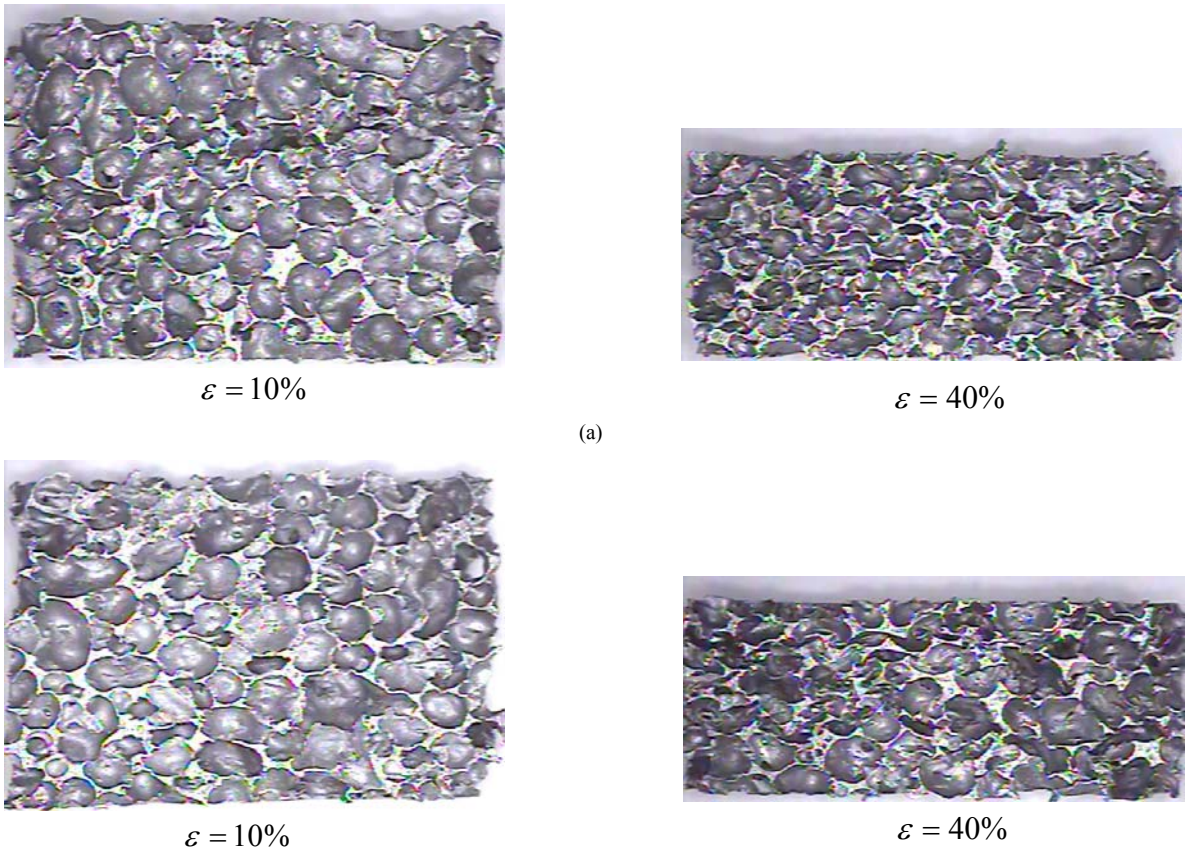

Fig 10. Deformation patterns at 10% and 40% strain (a) Monotonic compression, (b) Compression-compression fatigue

arisen due to the different cell morphology (cell shape, cell size etc.) of the finite element model from the real foam specimen.

On the other hand, the decreasing trend of elastic modulus in case of fatigue compression was found with strain unlike the DUOCEL and ALPORAS foam studied by Harte et al.[8]. Therefore the deformation mechanism of Al-Si-Ca alloy foam under the fatigue compression would be different from the monotonic compression. The drop of elastic modulus in case of fatigue compression is caused by the result of continuous cracking in damaged cell walls [8] due to the cyclic loading. Optical observation [Fig. 10 (b)] on the deformed specimen reveals that in case of fatigue compression some of the cells remained undeformed while many cells in weak areas became fractured after an incubation number of

cycles, which then broadened to the nearest weakest zone with additional fatigue cycles. It is also noticed that in the crush band the foam walls became disintegrated and rattled forming debris, which may reduce the stiffness of the foam.

5. CONCLUSIONS

The elastic modulus of the Al-Si-Ca alloy foam specimen has been found to increase with the monotonic compression while the unloading elastic modulus under fatigue compression showed a decreasing trend with increase of strain. The improved cruciform model along with the appropriate material properties of the foam cell wall measured indirectly by nondestructive nanoindentation method was developed to predict the compression behavior of closed cell aluminum alloy foam. The finite element analysis based on the improved cruciform model showed the same increasing behavior of unloading modulus with the increasing strain as in case of monotonic compression. The drop of elastic modulus in case of fatigue compression is caused by the result of continuous cracking in damaged cell walls due to the cyclic loading.

6. REFERENCES

1. P.S. Dubbelday, 1992, "Poisson's ration of foamed aluminum determined by laser doppler vibrometry", J. Acoust. Soc. Am.,91:1737-1744.
2. A. E. Simone, L.J. Gibson, 1998, "Aluminum foams produced by liquid state processes", Acta Mater, 46 : 3109-3123.
3. E. Andrews, S. Sanders, L.J. Gibson, 1999,"Compressive and tensile behavior of aluminum foams", Materials Science and Engineering A, 270 113-124.
4. A. E. Simone, L.J. Gibson, 1998, "The effects of solid distribution on the stiffness and strength of metallic foams", Acta Mater, 46: 3929-3935.
5. M. F Ashby, A.G Evans, L. J Gibson, J. W Hutchinson, N.A Fleck and H. G. N. Wadley, 1998, "*Cellular Metals: A Design Guide*", Butterworth Heinemann, pp. 92.
6. Kazi Tunvir, Amkee Kim, S. S. Cheon, 2005 Compressive behavior of cubic spherical FE model with wall thickness ratio, *Proc. 4th Int. Conf. on Porous Metals and Metal Foaming Technology (MetFoam'2005),* (Sept. 21st -23rd), Osaka, Japan.
7. Kazi Tunvir, Amkee Kim, "Crush behavior analysis of closed cell Aluminum alloy foam by cubic spherical model", Mechanics of Materials (going to be submitted in Journal of Mechanics of Materials).
8. A.M. Harte, N. A. Fleck and M.F., "Ashby:Fatigue failure of an open cell and a closed cellaluminum alloy foam", Acta Mater, 47 : 2511-2524.
9. *Handbook of Tables for probability and statistics*, 2nd ed. Abridged ed.
10. Amkee Kim, Kazi Tunvir, "Measurement of stress-strain relation for Al-alloy foam cell wall by instrumented nanoindentation method", Submitted to Journal of materials Letters.
11. Sugimura Y, Meyer J, He M.Y, Bart-Smith H, Grenestedt J, Evans A.G., 1997, "On the mechanical performance of closed cell foams", Acta Mater 45: 5245-5259.